A Compact Circular Polarized MIMO Fabric Antenna with AMC Backing for WBAN Applications

Tarannum U. Pathan, Bhagwat Kakde
Department of Electronics and Telecommunication, Madhyanchal Professional University, Ratibad, Bhopal, Madhya Pradesh, India

Corresponding author: Tarannum U.Pathan (e-mail: pathan.tannu24@gmail.com).

ABSTRACT A compact circular polarized (CP) multiple-input multiple-output (MIMO) fabric antenna with improved isolation at 2.4 GHz for wireless body area network (WBAN) applications is presented. A metamaterial (MTM)-inspired radiating element has been used for the miniaturization of the presented fabric antenna. The proposed antenna has very compact size of 58 x 23 x 1.6 mm^3. The circular polarization is achieved by trimming the two diagonal corners of the radiating elements. A defected ground structure (DGS) consists of two U-slots which is placed under each radiator to increase the bandwidth of the presented antenna. The isolation characteristics (S21) between the two antenna elements is increased by 20 dB by cutting a slit in a ground plane. The proposed CP-MIMO antenna incorporates an artificial magnetic conductor (AMC) layer to limit backward radiation towards the human body and hence enhances the gain. The proposed MIMO antenna has been designed on a denim substrate with permittivity ε_r =1.6 and thickness of 1.6 mm. The proposed antenna offers bandwidth of 160 MHz (2.38-2.54 GHz). The peak gain of antenna without AMC is 2.5 dBi and with AMC is 4.5 dBi. To validate the simulated results, a prototype for the proposed antenna has been fabricated and experimentally characterized. Due to its small size, low specific absorption rate (SAR), ease of integration and robustness, this antenna is a good option for wireless body area network (WBAN) applications.

INDEX TERMS Artificial Magnetic Conductor, Defected ground structure, MIMO Antenna, Isolation, Wearable antenna

I. INTRODUCTION

Continuous development in wireless electronic technology has enabled the integration of technology in cloth to enhance the capability. Such wearable textile antenna that can integrate into a communicating garment offer many potential applications, including military, telemedicine, GPS sensing for personal safety, wireless information relay, sports and tracking applications [1]. Circularly polarized (CP) antennas are attractive candidates for wearable applications due to their orientation flexibility, better mobility and multipath interference suppression capability. Multiple-input-multiple-output (MIMO) technology is also gaining popularity for improving link capacity, particularly in complex multipath environments. A multi-element antenna with circular polarization (CP) is a good choice for encountering multipath fading and establishing reliable channels [2,3]. However, the backward radiation resulting from wearable antennas has been a design challenge. Recently, several techniques for implementing the electromagnetic band gap (EBG) structures or artificial magnetic conductor (AMC) planes have been proposed to enhance the performance of wearable antennas. The AMC plane is used to eliminate the detuning effects, to increase the antenna gain and, meanwhile, reduce the back-lobe radiation as reported in [4,5,6,7]. Wearable textile antennas with different AMC backing structures have been reported in [4,5, 6,7]. However, these antennas are electrically large and radiation inefficient. The performance of wearable antenna in close vicinity to human body has been reported in [8].

It is important to mention that, the performance of wearable antenna is disrupted and drastically impair the resilience and reliability of wireless communication links due to multipath fading effects when it is smoothly stretched over the non-flat human body reported in [9,10]. Hence, MIMO antennas are widely suggested for improving communication performance. Many MIMO antennas for wearable applications have been reported in [10,11,12,13,14]. However, in previous demonstrations, the impact of antenna bending on its radiation characteristics has not been evaluated. More importantly, the backward radiation which is crucial to the operation of wearable antennas, has been largely overlooked. The textile MIMO antenna with high isolation using stub techniques have been reported

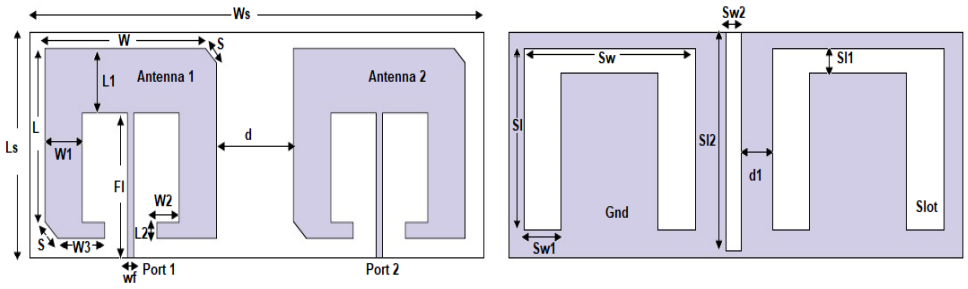

FIGURE 1. Proposed CP-MIMO Textile Antenna (a) Top View (b) Bottom View

TABLE I. Proposed Antenna parameter dimensions in mm

Parameters	L	W	Ls	Ws	L1	L2	W1	W2	W3	Fl	d	S	Wf	Sw	Sl	Sl1	Sl2	Sw1	Sw2	W3	d1
Dimensions (mm)	17.2	20.6	23	58	6.4	1.5	4.8	28	6	14.5	10	2.3	1	22	18	2.4	21.5	4.8	2.0	6.0	4

in [12,13,14]. The mutual coupling reduction between closely placed antennas in MIMO using meander line resonator has been reported in [15]. Despite the advancements in MIMO technology, all of the reported antennas are larger and have low isolation. As a result, obtaining compact and well-isolated antennas, while maintaining adequate performance, remains a challenging task.

In this paper, a wearable CP-MIMO textile antenna with AMC backing is reported that operates at 2.4 GHz in the industrial scientific and medical (ISM) band. The mutual coupling of the proposed antenna is as low as 25 dB over the entire band. Moreover, by using the AMC plane, the gain of the proposed antenna can be increased by 2 dBi and the backward radiation can be reduced down to 7 dBi.

II. ANTENNA DESIGN AND CHARACTERIZATION

A. DESIGN OF CP-MIMO FABRIC ANTENNA

Figure 1 depicts the diverse CP-MIMO textile antenna layout. The top aspect of the proposed antenna features two MTM-inspired radiators as shown in Figure 1(a). Figure 1(b) shows the bottom aspect of antenna which consists of two inverted U-slots below each antenna element in the ground. Furthermore, a slit in the ground is placed between both antenna elements to enhance isolation (S21) characteristics. This MIMO antenna system consists of two extremely close-spaced antenna elements. In the y-axis direction, the two antenna elements are separated by 10 mm (0.08λ). Each antenna element size is 17 x 20 mm^2.The antenna has been designed on a denim substrate of permittivity (ε_r =1.6) with 1.6 mm thickness [12,13]. As illustrated in Figure 1(a), a second antenna with same geometry is placed with a common ground plane. Using slotting DGS techniques, a minimum spacing of 0.08λ is achieved between two extremely close-spaced antenna elements. Table I shows the parameters of the presented antenna in mm.

B. DESIGN OF FABRIC MIMO ANTENNA WITH AMC

The proposed CP-MIMO fabric antenna is backed with a 2×4 AMC array of size 23 × 74 mm^2. The unit cell dimensions are shown in Figure 2 (a). The AMC unit cell is made of denim material. The coatex conductive fabric with a conductivity of 1.2 x 10^7 S/m is used for the radiating element, unit cells, and ground plane. The plating material of coatex is nickel–copper–nickel with 100% woven polyester.

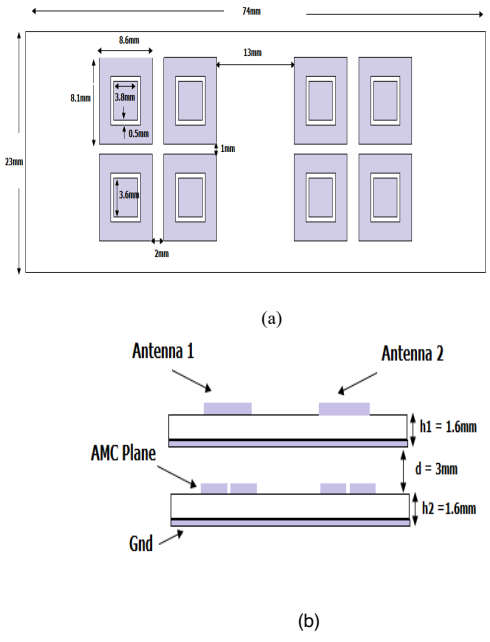

FIGURE 2. (a) AMC dimensions (b) Cross-section view of the proposed antenna with AMC

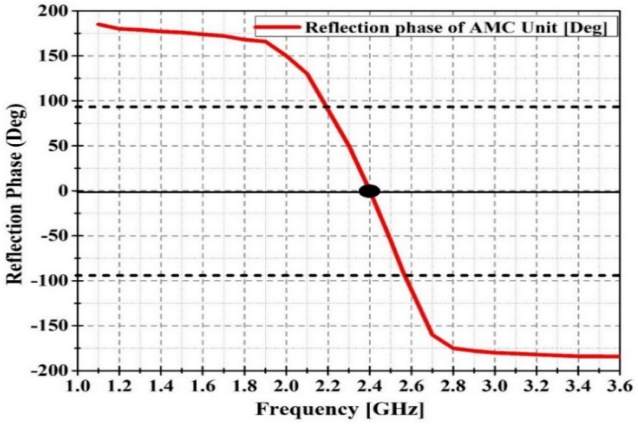

FIGURE 3. Reflection phase of the AMC unit cell.

The reflection phase frequency response of the AMC unit cell varies from $+180^0$ to -180^0 over the band from 1 GHz to 3.6 GHz with zero-crossing at an odd symmetry around 2.4 GHz. This phase response is quasi-linear from about 2.1 GHz to 2.7 GHz. The reflected wave is nearly in anti-phase at 2.4 GHz which is shown in fig.3. The AMC unit cell operating bandwidth is 380 MHz, which can be computed from $+90^0$ to -90^0 on either side of 2.4 GHz.

C. PROTOTYPE OF AMC-BACKED CP-MIMO FABRIC ANTENNA

Figure 4 shows the top view and bottom view of the prototype fabric antenna. The fabricated AMC unit cells of size 2x4 have been shown in Figure 4(c). The antenna structure is cut with help of heavy duty cutter knife blade and a sizer cutter. Then due adhesive of coatex conductive fabric is directly placed on jeans cloth material.

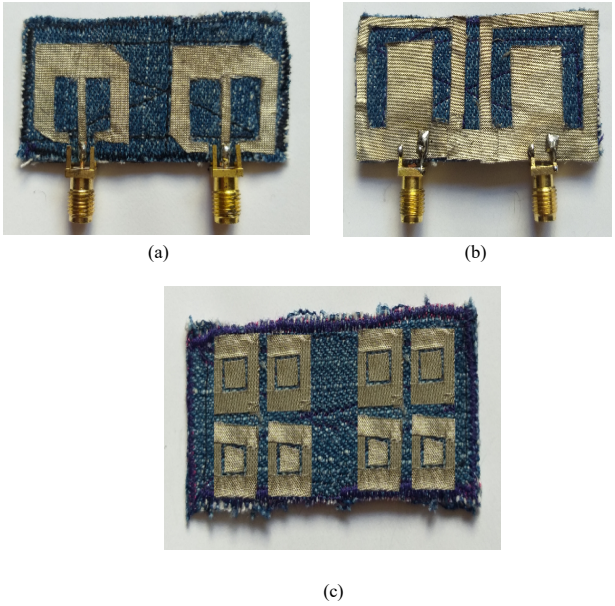

(a) (b)

(c)

FIGURE 4. Fabricated fabric CP-MIMO antenna (a) Top view (b) Bottom view (c) AMC Unit Cell

III. RESULTS AND DISCUSSION

The simulation of the proposed antenna has been performed using ansys HFSS software. The two inverted U-slots in the ground are initially introduced in the first stage, i.e., without slit DGS, and then modified by the slit inserted between the two inverted U-slots in the second stage, i.e., with slit DGS. The compact MIMO antenna with high isolation is always desirable. Isolation (S21) characteristics means how much power comes out of one antenna, assuming the other antenna is excited.

Figure 5 (a) and 5 (b) gives the MIMO-CP surface current distribution with and without a ground slit at resonant frequency achieved by exciting antenna 1 and terminating antenna 2 by a matched load, respectively. When the two patches are arranged on a ground with no slit, a high current is induced on the right side of the coupled antenna element. Figure 5 (a) shows that without slit, some of the surface current is coupled from antenna-1 to antenna-2. The proposed antenna with slit reduces the high mutual coupling between the antenna parts. In the case of a MIMO-CP antenna with a slit, the current is especially focused at the corners of the right-side patch and there is no current on the left-side patch, as shown in Figure 5 (b). The magnetic field is trapped within the ground slit as a result of this phenomenon, it prevents the surface current from flowing further. As a result of using a slit, electromagnetic energy is prevented from propagating from antenna-1 to antenna-2, resulting in a high level of isolation.

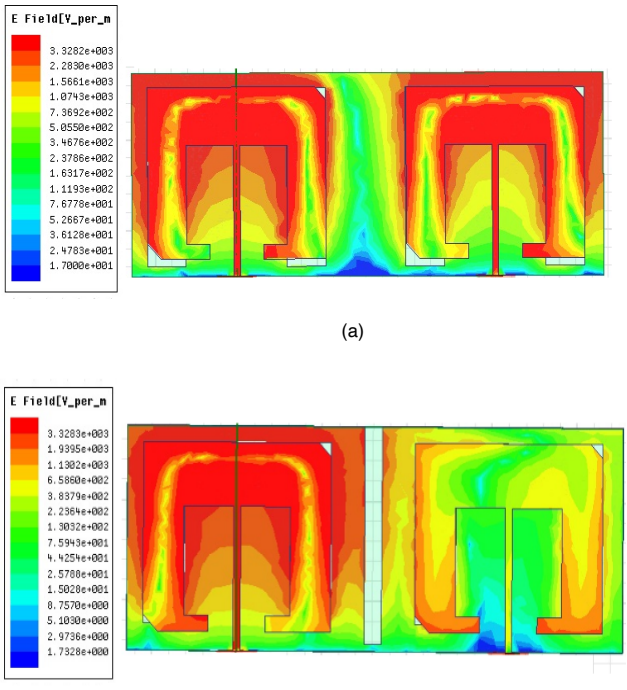

(a)

(b)

FIGURE 5. Fabric CP-MIMO antenna (a) without slit DGS (b) With Slit DGS

The isolation (S21) characteristics of MIMO antenna with and without DGS slit technique is depicted in figure 6 (a). When the inverted U-slot in the ground plane is employed, the CP-MIMO antenna without the slit in DGS has poor isolation in the whole 2.4 GHz band. By modifying the DGS ground plane with slit technique, it improved isolation S21 up to 20 dB at 2.4 GHz. Furthermore, the S21 is enhanced by 15 dB at 2.4 GHz due to AMC-backing in the presented design, as illustrated in Figure 6 (b).

The addition of a slit in the DGS achieves good isolation. It demonstrates that adding a slit in DGS results in more than 20 dB isolation.

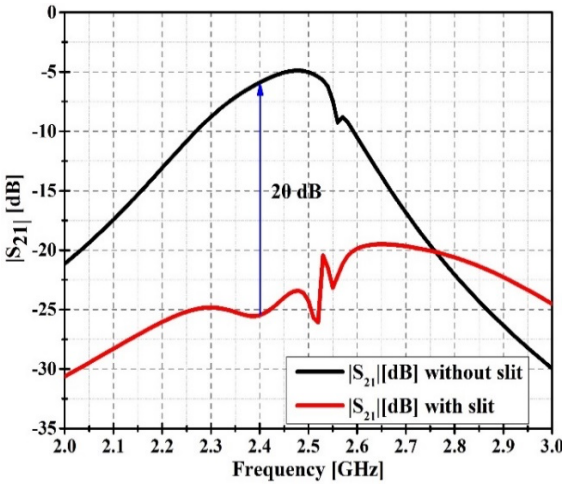

(a)

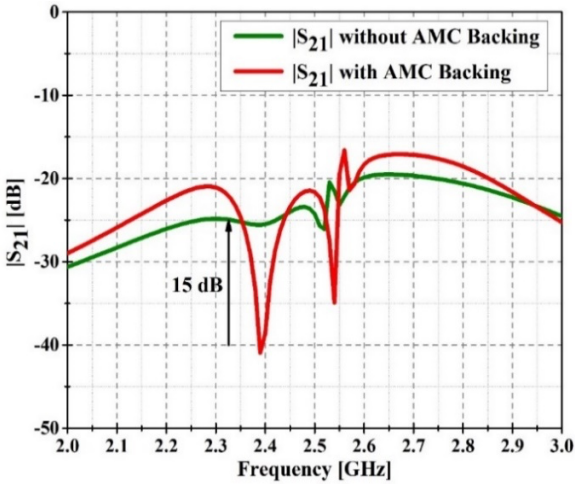

(b)

FIGURE 6. Effect of slit & AMC on S_{21} (a) With and without slit (b) With and without AMC

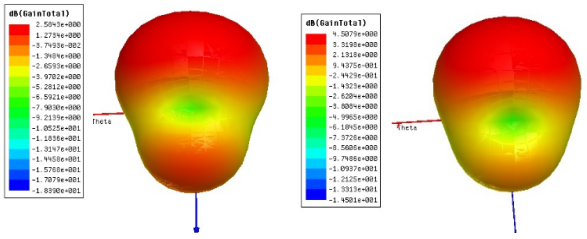

FIGURE 7. Gain of proposed Antenna (a) Without AMC-backing (b) With AMC-backing

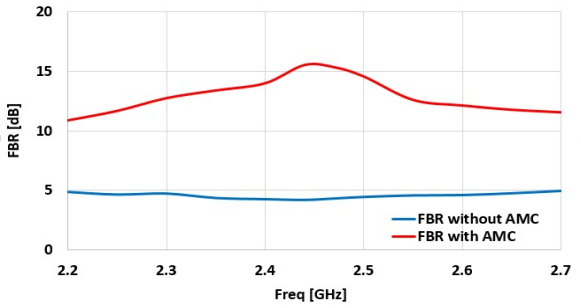

FIGURE 8. Front to Back Ratio (FBR) of the proposed antenna with and without AMC structure

Figure 7 shows the gain of the CP-MIMO antenna with and without AMC. It can be shown that using AMC, the gain is enhanced up to 2.5 dB. Figure 8 shows the front to back ratio (FBR) of the CP-MIMO antenna with and without AMC. The FBR is enhanced up to 10 dB at 2.45 GHz. From table II, it is evident that, the proposed CP MIMO antenna with AMC structure has better performance than without AMC structure.

TABLE II. CP-MIMO antenna with and without AMC-backing.

Results	Without AMC	With AMC
Frequency [GHz]	2.4	2.4
Bandwidth [MHz]	130	160
Isolation S_{21} [dB]	-25	-40
Gain [dB]	2.5	4.5
Eficiency [%]	79.2	85.6
Backward Radiation [dB]	-1.7	-9.4

Figure 9 depicts the simulated versus measured results of the proposed CP-MIMO fabric antennas with AMC-backing. The proposed MIMO antenna offers bandwidth of 160 MHz (2.39 -2.55 GHz), which fully covers the 2.4 GHz WBAN spectrum. The simulation of proposed antenna is carried out in free space.

Both port 1 and port 2 of the proposed CP MIMO textile antennas offer bandwidth of 160 MHz. The S-parameters |S11|& |S22| is below -15 dB at 2.4 GHz. Figure 9 (b) concludes that isolation S21 is obtained below 24 dB over the entire operating band with AMC-backing. The axial ratio (AR) is critical for assessing CP performance, therefore the AR values are depicted in Figure. 9 (c).

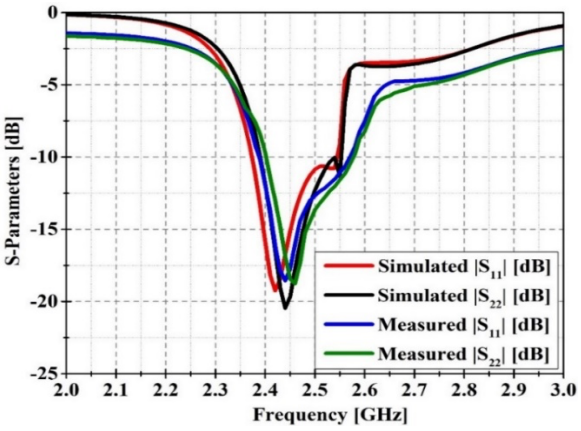

(a)

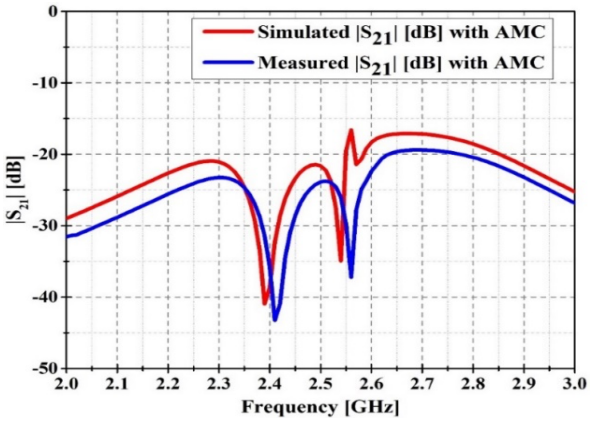

(b)

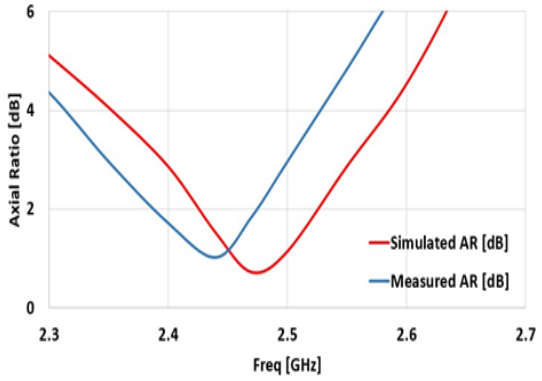

(c)

FIGURE 9. Simulated vs. Measured Results (a) S11 and S22 (b) S21 and (c) Axial Ratio (AR)

The antenna with whole torso model is more complicated that is why here antenna is computed in free space.
It can be seen that proposed antenna offers AR bandwidth of 160 MHz (2.34 -2.50 GHz). Figure 10 depicts the simulated versus measured radiation pattern of the proposed CP MIMO fabric antenna.

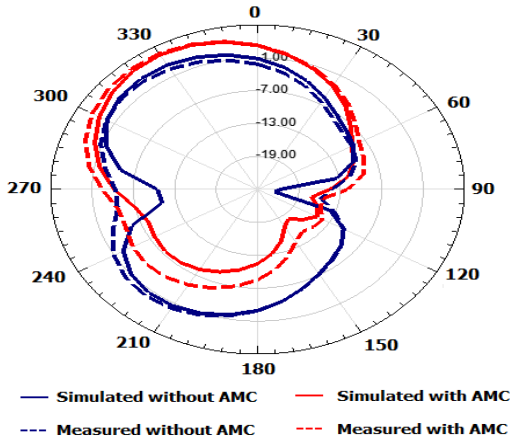

(a)

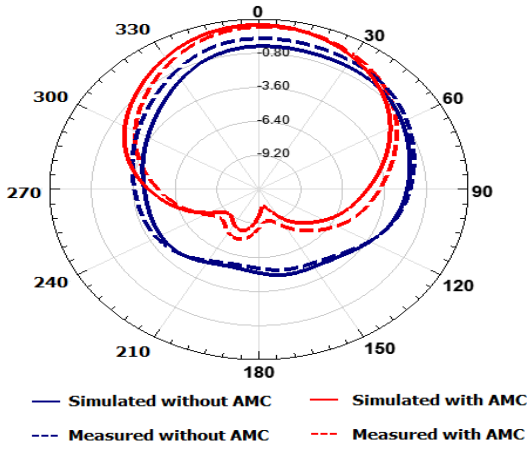

(b)

FIGURE 10. Radiation patterns of the proposed CP MIMO antenna with AMC at 2.45 GHz simulated vs. measured (a) E-Plane (b) H-Plane

A. ANTENNA PERFORMANCE ANALYSIS

1) BENDING ANALYSIS:

The feasible utilization of the investigated antenna in bendable and flexible devices demands to estimate its performance in bent configurations. Therefore, the investigated CP-MIMO fabric antenna is curved in the X-directions for different radii R1 = 50 mm, R2= 60 mm, and R3 = 70 mm. To justify the S11 parameter, the measurement has been carried out on a foam cylinder with radii of R1 = 70 mm, R2 = 60 mm, and R3 = 50 mm as illustrated in Figure 11.

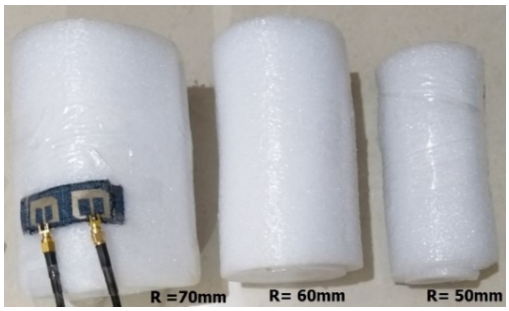

FIGURE 11. Bending evaluation on different radii (Rx) in mm

TABLE III. Analysis of bending performance

Bending along X-axis				
Rx in mm	Flat	70 mm	60 mm	50 mm
Gain in dBi	4.5	4.4	4.3	4.1
Efficiency [%]	85.6	81.2	79.3	77.5

The return loss of the proposed antenna at various bending angles is shown in the Figure 12(c). Performance characteristics are similar to an identical antenna in planar arrangement as shown in Figure 12 (a). This particular observation indicates the robustness of the proposed design against severely curved topological conditions, which are typical in human wearable antennas.

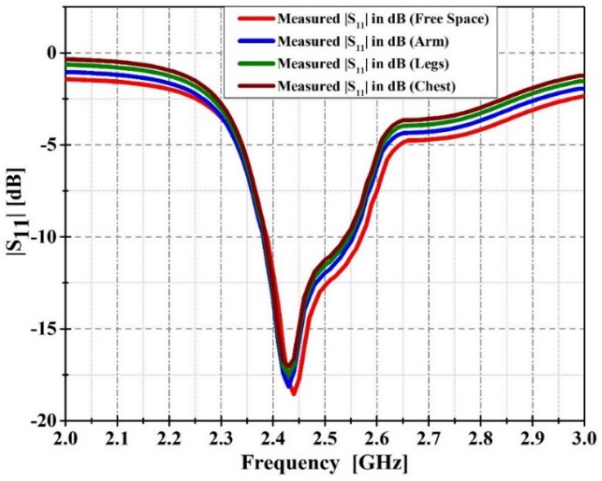

(a)

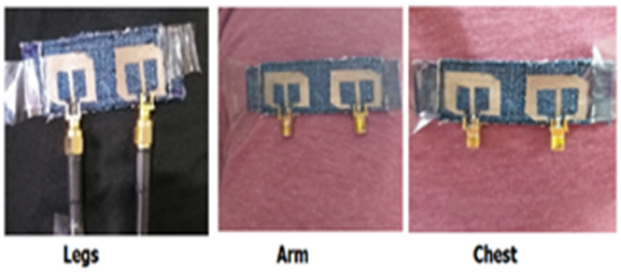

(b)

(c)

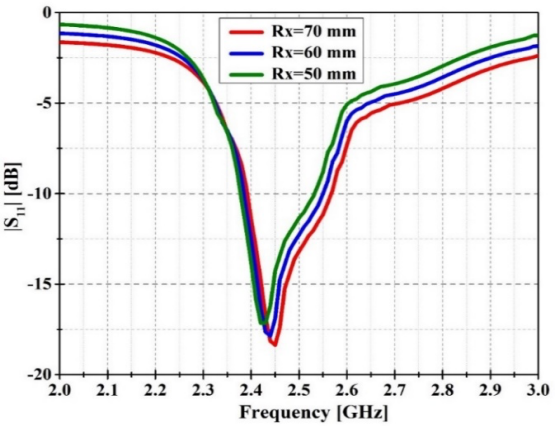

FIGURE 12. Bending Analysis (a) S11 on several human body parts (b) tested on legs, arm and chest and (c) S11 on various bending angle

Further to that, the antenna has been tested on several parts of the body, i.e., chest, leg, and arm, in order to evaluate the performance in close-to-realistic wearable scenarios. The fabricated prototype of the investigated antenna was arranged on a real human body to study the impact of the human body, as illustrated in Figure.12 (b). The stable performance characteristics was observed as shown in Figure.12 (a).

B. SAR ANALYSIS:

To analyse the effect on the human body, the antenna is kept on a human tissue model with a 1 mm gap, which consists of four-layer box (100 mm x 100 mm), including skin, fat, muscle, and bone as seen in Figure 13 (a). Table IV lists the material characteristics at 2.45 GHz for the four layers, with thicknesses of 2, 5, 20, and 13 mm, respectively.

TABLE IV. Material characteristics of human biological tissue

	Skin	Fat	Muscle	Bone
Permittivity (ε_r)	36.89	5.28	52.67	18.49
Conductivity (S/m)	1.48	0.11	1.77	0.82
Density (Kg/m^3)	1001	900	1006	1008

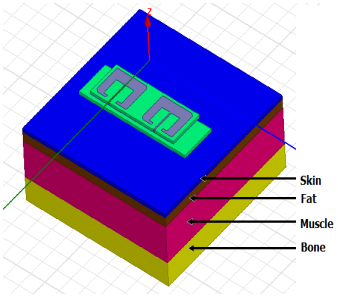

(a)

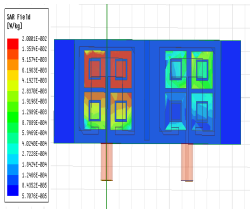

(b)

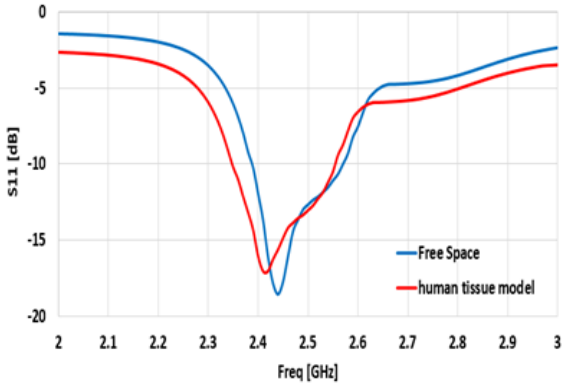

(c)

FIGURE 13. Simulated 1-g averaged SAR distributions (a) SAR Human Model (b) 1-g SAR values (c) S11 Free space Vs humun tissue model

The reference input power of 100 mW produces SAR distribution as shown in Figure 13. The simulated SAR value of antenna are 0.02 W/kg for 1 g of tissue at 2.45 GHz which is substantially below the FCC limit of 1.6 W/kg. The resonant frequency of the antenna gets slightly affected when mounted on the human tissue model.

C. MIMO PERFORMANCE:

The ECC can be calculated using *S*-parameters using the following formula [16]

$$ECC = \frac{|S_{11}^{*}S_{12} + S_{21}^{*}S_{22}|^2}{(1-|S_{11}|^2-|S_{21}|^2)(1-|S_{22}|^2-|S_{12}|^2)} \quad (1)$$

As shown in Figure 14, the ECC value of MIMO antenna is less than 0.01 over the operating band.

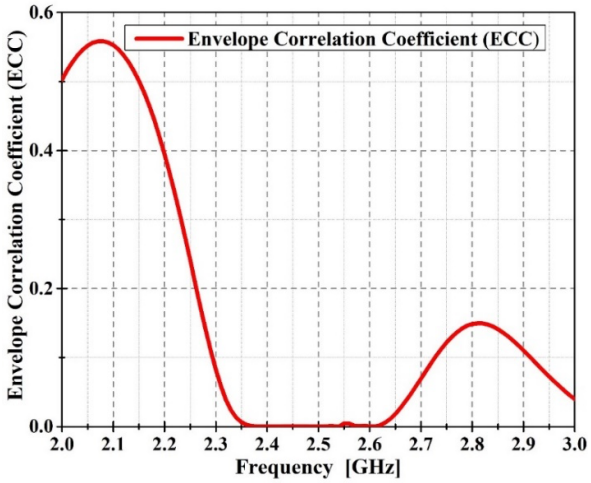

FIGURE 14. The simulated ECC of CP-MIMO fabric antenna

TABLE V. Comparison of the presented work to other state-of-art designs

Ref	Size (mm*mm*mm)	Dielectric Const. (ε_r)	No. of AMC cells	Gain (dBi)	FBR (dB)	SAR (W/kg)	MIMO
[4]	$1.2\lambda_0$ x $1.2\lambda_0$ x $0.03\lambda_0$ (150x150x3)	1.7	3x3	1.5	7.0	0.02	No
[5]	$0.4\lambda_0$ x $0.6\lambda_0$ x $0.04\lambda_0$ (50x75x5)	1.2	2x3	NA	12.8	0.54	No
[6]	$0.34\lambda_0$ x $0.5\lambda_0$ x $0.07\lambda_0$ (42x63x8)	1.6	2x3	5.0	12.0	0.34	No
[7]	$0.8\lambda_0$ x $0.8\lambda_0$ x $0.05\lambda_0$ (100x100x6)	1.2	4x4	2.4	11.0	0.04	No
[8]	$0.3\lambda_0$ x $0.9\lambda_0$ x $0.03\lambda_0$ (16x46x1.6)	1.5	Not Used	2.0	11.5	NA	No
[12]	$0.36\lambda_0$ x $0.56\lambda_0$ x $0.015\lambda_0$ (35x55x1.6)	1.6	Not Used	2.8	10.0	NA	Yes S21 = 26 dB
[13]	$0.5\lambda_0$ x $0.8\lambda_0$ x $0.04\lambda_0$ (60x97x1.4)	1.6	Not Used	2.0	11.5	1.0	Yes S21 = 22 dB
[14]	$0.32\lambda_0$ x $0.70\lambda_0$ x $0.015\lambda_0$ (40x86x1.6)	1.6	Not Used	2.8	12.2	NA	Yes S21= 25 dB
Proposed Work	$0.19\lambda_0$ x $0.59\lambda_0$ X $0.05\lambda_0$ (23x74x6)	1.6	2x4	4.5	14.0	0.02	Yes S21 = 40 dB

D. *COMPARISON WITH OTHER STATE OF THE ART DESIGNS*

To study the novelty of this work, the suggested MIMO textile antenna has been compared with the current state-of-the-art designs. Table V shows the comparison of various antennas available in the existing literature along with the proposed work. It compares the performance of the investigated CP MIMO antenna to the previously published antenna design with AMC. It concludes that the proposed antenna has a smaller size compared with the designs reported in [4-7] and [12-14]. The presented antenna offers higher isolation S21 and FBR than the reported designs in [11-13]. Also a good gain and low SAR is obtained in the proposed fabric antenna design.

IV. CONCLUSION

A compact CP-MIMO fabric antenna with AMC integration is presented for WBAN applications. The miniaturization of the proposed CP-MIMO fabric antenna is achieved by employing metamaterial-inspired radiator with an 80% size reduction. To increase the bandwidth of the proposed antenna, a DGS with two U- slots is added below each radiator. The isolation performance is improved by adding one slit in between two U-slots in the shared ground plane. The isolation S21 of the MIMO antenna with AMC is 40 dB at 2.4 GHz. The proposed CP MIMO fabric antenna offers bandwidth of 160 MHz. The overall dimension of the proposed antenna with AMC is 23 x 74 x 1.6 mm^3. The proposed antenna has very low backward radiation and good gain of 4.5 dBi is observed. The MIMO antenna element with closely coupled spacing of 0.08λ provides exceptionally good port isolation of more than 24 dB throughout the entire operating band. Because of its compact size and better isolation, the recommended CP MIMO antenna is suitable for WBAN applications.

REFERENCES:

[1] M. S. Shakhirul and A. H. Ismail, "Textile antenna with simultaneous frequency and polarization reconfiguration for WBAN," *IEEE Access*, vol.6, no.6, pp.7350-7358, Dec 2018.

[2] F. A. Dicandia, S. Genovesi, and A. Monorchio, "Analysis of the performance enhancement of MIMO systems employing circular polarization," *IEEE Trans. Antennas Propag.*,vol. 65, no. 9, pp. 4824-4835, Sep 2017.

[3] A. Iqbal, A. Smida, A. J. Alazemi, M. I. Waly, N. K. Mallat, and S. Kim, "Wideband circularly polarized MIMO antenna for high data wearable biotelemetric devices," *IEEE Access*, vol. 8, pp. 17935-17944, Jan 2020.

[4] S. Velan and M. Kanagasabai, "Dual-band EBG integrated monopole antenna deploying fractal geometry for wearable applications," *IEEE Antennas and Wireless Propagation Letters*, vol. 14, no. 2, pp. 249-252, Sept 2015. doi:10.1109/LAWP.2014.2360710

[5] A. Mersani, J. Ribero and O. Lotfi (2018, March).Improved radiation performance of textile antenna using AMC surface. Presented at 15th International Multi-Conference on Systems, Signals, and Devices (SSD), pp.627-631, doi:10.1109/SSD.2018.8570488

[6] A. Mersani, J. Ribero and O. Lotfi, "Design of a textile antenna with artificial magnetic conductor for wearable applications," *Microwave and Optical Technology Letters*, vol 60, pp.1343-134, June 2018, doi:10.1002/mop.31158

[7] S. Yan, P. J. Soh and G. A. E. Vandenbosch, "Low-profile dual-band textile antenna with artificial magnetic conductor plane," in *IEEE Transactions on Antennas and Propagation,* vol. 62, no. 12, pp. 6487-6490, Dec 2014, doi: 10.1109/TAP.2014.2359194

[8] K. Wang and J. Li,Jeans(2018, Dec).Textile Antenna for Smart Wearable Antenna. Presented at 12th International Symposium on Antennas, Propagation and EM Theory (ISAPE), pp.1-3, doi:10.1109/ISAPE.2018.8634337

[9] T. Hassan, M. U. Khan, H. Attia, and M. S. Sharawi, "An FSS based correlation reduction technique for MIMO antennas," *IEEE Trans. Antennas Propag.*, vol.66, no.9, pp.4900-4905, May 2018, doi:10.1109/TAP.2018.2842256

[10] L. Qu, H. Piao, Y. Qu, H.-H. Kim, and H. Kim, "Circularly polarised MIMO ground radiation antennas for wearable devices," *Electronics Letters*, vol.54, no.4, pp.189-190, Dec 2018, doi:10.1049/el.2017.4348

[11] H. Li, S. Sun, B. Wang, and F. Wu, "Design of compact single-layer textile MIMO antenna for wearable applications," *IEEE Trans. Antennas Propag.*, vol. 66, no. 6, pp.3136-3141, March 2018.

[12] A.K.Biswas, and U. Chakraborty, "Compact wearable MIMO antenna with improved port isolation for ultra-wideband applications", *IET Microw. Antennas Propag,* vol. 13, no. 4, pp. 498-504, Feb 2019. doi:10.1049/iet-map.2018.5599

[13] S. Roy, S.Ghosh, S.Pattanayak, and U.Chakarborty, "Dual-polarized textile-based two/four element MIMO antenna with improved isolation for dual wideband application", *Int J RF Microw Computer Aided Eng.*, pp.1-20, May 2020.doi: 10.1002/mmce.22292

[14] T. Ashtankar and N.K. Choudhari, "Design and analysis of a compact MIMO textile antenna with improved mutual coupling for WBAN applications," *IOSR Journal of Electrical and Electronics Engineering*, vol. 15, no. 2, pp. 8-13, April 2020. doi: 10.9790/1676-1502020813.

[15] H. Jiang and J. Ding, "Broadband extremely close spaced 5G MIMO antenna with mutual coupling reduction using metamaterial-inspired superstrate" *Opt Express*. vol.27, no.3, pp.3472-3482, Feb 2019., doi:10.1364/OE.27.003472. PMID: 30732367.

[16] S. Kumar and D. Nandan, "Wideband circularly polarized textile MIMO antenna for wearable applications," *IEEE Access*, vol. 9, pp. 108601-108613, July 2021, doi: 10.1109/ACCESS.2021.3101441.